International Journal of Grid and Distributed Computing
Vol. 13, No. 2, (2020), pp. 246-252

Strutural, Dielectric and Magnetoelectric Properties of Fe^{+3} doped $BaTiO_3$

Manoj Baloni
Department of Physics SGRR(PG) College Dehradun

Abstarct:

$BaTi_{1-x}R_xO_3$(whereR=Fe;x=0.0,0.4,0.6) have been synthesized by solid-state reaction technique. The powders have decarbonated at1200 ºC and sintered at 1250 ºC for 2 hours. The study reveals that the coexistence of tetragonal and hexagonal phases is strongly influenced by Fe doping concentration. The increase in crystallite size, lattice strain, c/a ratio and grain size has been found with Fe doping.The dielectric constants of Fe-doped $BaTiO_3$ multiferroic ceramics exhibited a decrease with Fe concentration.The decrease of dielectric losswith increasing frequency is attributed to the fact that thefrequency of charge carriers cannot follow the changes to the externally applied electric field beyond a certain frequency limit.Overall, iron (Fe) doping has remarkably influenced the structural, morphological, electrical and dielectric properties of barium titanate (BaTiO3)ceramics.Magneto dielectric behavior may be due to the coupling between ferroelectric and magnetic domains.Magneto dielectric coefficient increases with Fe doping concentrationthusshowing multiferroic nature.

Keywords: *Ceramics, Barium titanate, Multiferroic, Magneto dielectric Coefficient, Dielectric properties.*

Introduction:

Multiferroic composites are of immense interests for studies on the physics of electromagnetic coupling and for use in a variety of applications.Composites consisting of two or more phases are of importance for control of either a specific physical property or for achieving new properties or functionalities that are absent in the constituent phases.$BaTiO_3$ (BTO) is most preferred due to its stable structure with high degree of functionality. It hasa ABO_3 type structure where A and B are cations of different sizes, with the 6 fold coordinate B cation in the middle, the 12 fold coordinate A cation in the corner and the anion, commonly oxygen, in the centre of the face. The phase of $BaTiO_3$ at room temperature is tetragonal and it transforms to cubic phase above 130ºC. It also exists in orthorhombic phase at 0ºC and in rhombohedral phase below -90ºC. Above 1460ºC, $BaTiO_3$ exits in hexagonal phase. BaTiO3 is the most frequently utilized ferroelectric material and high dielectric constant and low dielectric loss makes it one of the promising candidates for dynamic random-access memory (DRAM) and tunable microwave device applications. BaTiO3 exhibit lower ionic conductivity and behaves as an insulator at room temperature. The substitution of acceptor impurities at Ti-sites improves both ionic and electronic conductivity accompanied by the formation of charge carriers and oxygen vacancies. The most considerable increase of the electrical conductivity is achieved by Fe substitution. The Fe ions generally substitute for Ti^{4+}in $BaTiO_3$ceramics. The ferroelectric properties of $BaTiO_3$ can be efficiently controlled by doping with different doping elements. Ferroelectricity usually occurs when the metal ions have empty d- orbitals (Ti^{+4} in case of $BaTiO_3$) while partly filled d level ions are required for magnetism to occur in transition metal ions. Fe doped $BaTiO_3$ system may offer an interesting combination of ferroelectric and magnetic characteristics. Most of the studies on Fe doped bulk BaTiO3 focus on structural, dielectric andmicro structural properties. Fe doped$BaTiO_3$(BT) materials in the bulk form are still explored over a wide range of compositions and controlled ion substitutions. Few reports are available on this issue where the micro-structural changes in Fe doped barium titanate [1-11], dielectric characteristics of Fe-ion doped $BaTiO_3$ (Fe is doped at Ti-site), exaggerated grain growth in Fe doped $BaTiO_3$ to study hexagonal phase in $BaTiO_3$ dielectric characteristics of BT co-doped [12-13] with Fe , electrical transport properties of Fe doped BT at high temperature[14], valence change and phase stability of Fe doped BT annealed in O_2 and H_2 are discussed. In this paper, the synthesis, characterization and dielectric properties of Fe-doped

ISSN: 2005-4262 IJGDC

BT have been studied and the effect of magneticfield on the dielectric properties of Fe doped BT has been analyzed.

Synthetic Procedure:

$BaTi_{1-x}R_xO_3$(whereR=Fe;x=0.0,0.4,0.6) were prepared bysolid state reaction method, using required amountof analytical grade reagents $BaCO_3$, TiO_2, Fe_2O_3 as starting materials. The oxides were well-mixed in acetone and grounded in an agate mortar for several hours until a dried powder was obtained. The calcinations step was performed at temperatures at 1200°C for 2 h. The calcined powder was pressed by uniaxial hydraulic press at a pressure of ~31.2×10^6 Pa into cylindrical pellets of 1-2 mm thick and 8 mm diameter. These pellets were then sintered at 1250°C for 5 h. The powder of sintered pellets was carried out by X-ray diffractometer (Brucker D8 Advance) using Cu-K_α radiation (λ = 1.5418Å) for Crystal structure and phase identification. The microstructure and the composition analysis were investigated using FE-SEM (FEI, Quanta 200). The Sintered pellets were polished for smooth parallel faces and coated with silver paste to ensure good ohmic contact and then dried at 120°C for 30 min, before taking electrical measurements. Dielectric measurements were conducted on an automated HIOKI 3532-50 Hi Tester, LCR meter. Magneto dielectric properties were studied using dielectric spectrometer attached to an electromagnet with maximum field 9kOe.

Results and Discussion:

The XRD pattern of the samples with the Fe concentration is shown in Fig.1. Pure BT XRD pattern show a single-phase tetragonal structure without any evidence of an impurity phase.As the concentration increasesfrom x=0.0 to x=0.6 the compositions exhibit a mixture of both tetragonal and hexagonal phases.The hexagonal phase dominates with increasing Fe doping concentration.The phase formation in $BaTi_{1-x}Fe_xO_3$ ceramics is also dependent on the calcinations as well as sintering temperature [15]. X-ray diffraction (XRD) pattern of powder of all the sintered samples show that diffraction peaks occurred at slightly smaller angles and, although appreciable scatter existed in the *c*-axis values, the data did seem to indicate a lengthening of the *a*-axis and shortening of the *c*-axis to produce a more cubic structure with little change in cell volume. XRD patterns of higher concentration of Fe^{+3} doped BT samples, could be thought that the patterns fit well with the peak position of Standard BT phase[15].

ISSN: 2005-4262 IJGDC

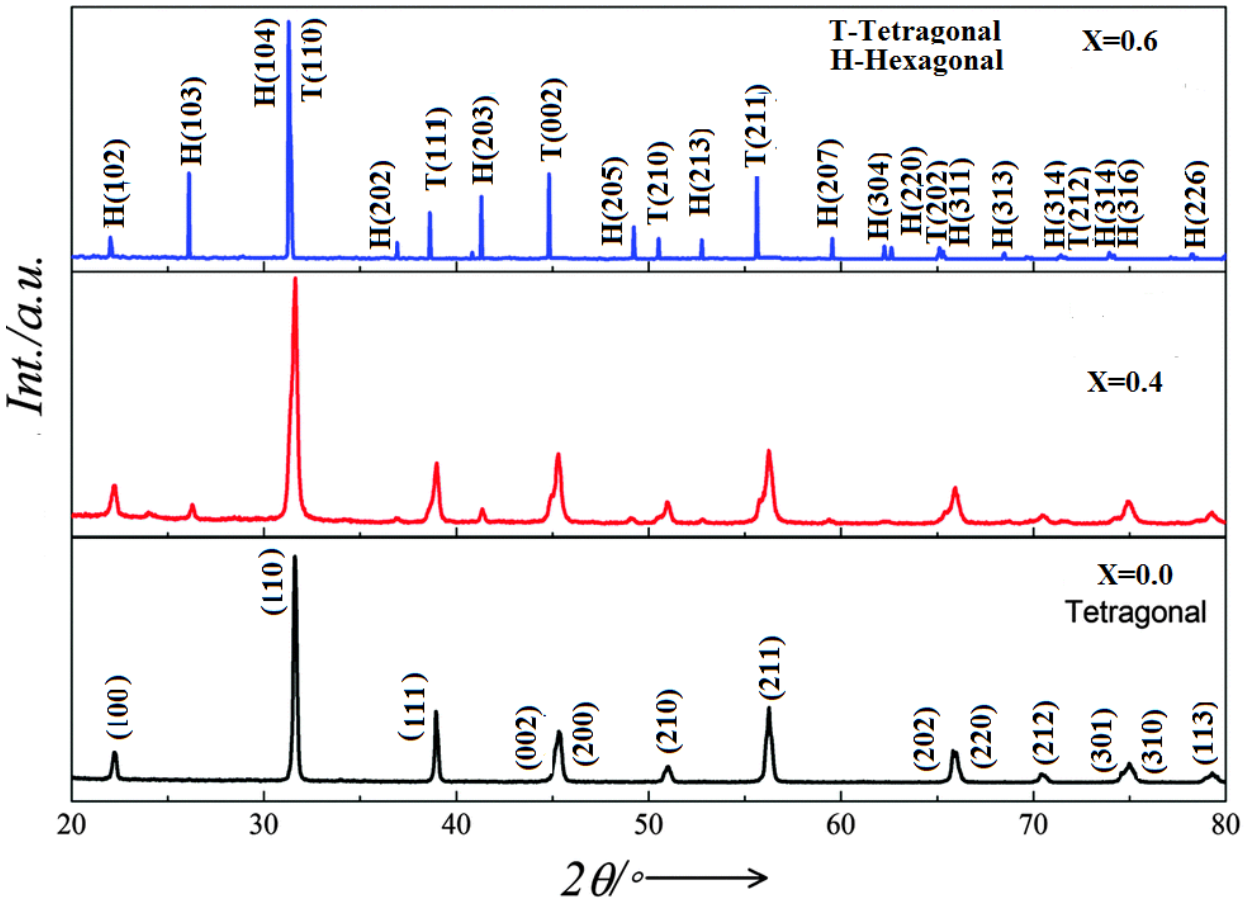

Fig. 1. XRD patterns $BaTi_{1-x}Fe_xO_3$for (x=0.0, 0.4 and 0.6)

The linear particle size (L) and lattice strain (η) was calculated using following Scherrer's equation[16] and data is given in Table 1.$\beta_{1/2}\cos\theta = K\lambda/L+\eta\sin\theta$where K = 0.89, $\beta_{1/2}$ is full width at half maxima. The lattice strain was calculated from slope of $\sin\theta$ versus $\beta_{1/2}\cos\theta$ plot. From the data it is observedthat Fe doping increases the crystallite size, unit cell parameters and lattice stain in BT, which may be due to replacement of large ionic radii Fe^{+3} (r_6^{2+} =0.645 Å) ion relative to smaller Ti ion (0.605Å).

Table 1—Structural and dielectric properties of $Ba_{1-x}Fe_xTiO_3$

	Tetragonal Phase		Hexagonal Phase				
X	a(A)	c(A)	a(A)	c(A)	Grain size((μm)	Strain (η)	δ
0.0	4.1110	4.1115	-	-	1.6	1.24	29.08
0.4	4.1140	4.1090	5.6585	13.5599	2.7	1.34	37.20
0.6	4.1155	4.1030	5.6597	13.5620	3.0	1.42	40.20

The FE-SEM images of $BaFe_{1-x}TiO_3$ for x = 0.0, 0.4, 0.6 respectively are shown in Fig. 2. From the SEM micrographs it is clear that microstructure, grain growth and grain size of all $BaTiO_3$ samples are decisively affected by the composition as well as the percentage of the structural transformation from tetragonal to hexagonal phase. The surface morphology of prepared samples is uniform and dense. The grain size with the Fe composition BTO samples increases from x=0.0 to x=0.6. The average grain size was determined by classical linear interception method and the data is presented in Table 1. From the data it is found that grain size increase with Fe doping. The grain size of pure BT is uniform and surface

ISSN: 2005-4262 IJGDC

appear as well-distributed crystallites[17]. FE-SEM image at x=0.4 is composed of mainly two types of grains, having rectangular and hexagonal shapes,while at x=0.6, mostly hexagonal grains are seen.

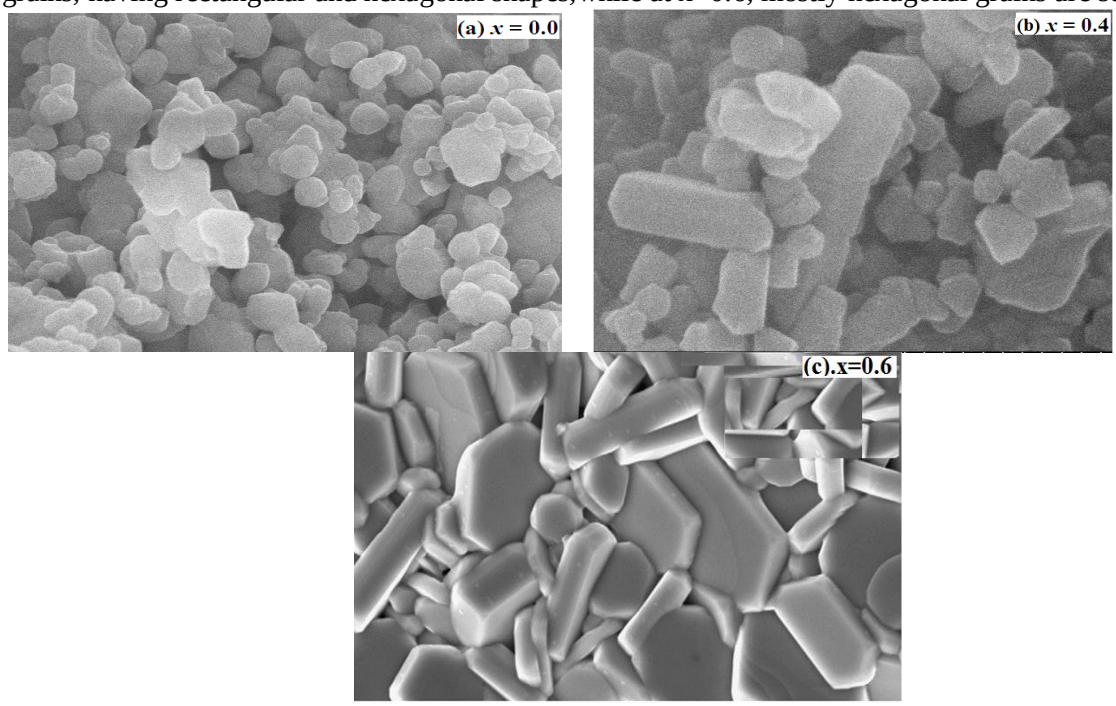

Fig. 2—FE-SEM images of $Ba_{1-x}Fe_xTiO_3$ (a) x = 0.0(b) x = 0.4 (c) x = 0.6

The variation of relative dielectric constant ($\epsilon' r$) and dielectric loss (tanδ) of BTO samples with frequency at room temperature for different compositions is shown in Fig. 3. It is evident from the Fig. 3 that both relative dielectric constant and dielectric loss decrease upto10^4 Hz. The relative dielectric constant remains almost constant with frequency in the range of 10^4–10^6 Hz. It is observed from Fig. 3(a) that the dielectric constant was high at low frequency may be due to dislocations, voids and defects present in the crystal structure. Also, the high dielectric constant can be directly associated with the presence of grains and interfaces. The fast decrease of the relative dielectric constant in the low- frequency region (below 10^4 Hz), is attributed to the space charge polarization or interfacial polarization induced by the structural defect such as oxygen vacancies ,and the coexistence of Fe^{+3} ions in the Fe-doped BTO ceramics[18]. As Fe concentration x increases the dielectric constantdecreases significantly. The decrease in dielectric constant with Fe substitution can be attributed to the creation of oxygen vacancy due to Fe^{+3} ions replacing Ti^{+4} ions. Such oxygen vacancy leads to the breaking of co-operative vibration of Ti-O bonds, which affects the dielectric properties. Fe in $BaTiO_3$ acts as an acceptor, leads to increase the conduction mechanism and hence a reduction in the dielectric constant values. As the frequency increases, some of them are not able to follow the alternating field and may have less contribution to $\epsilon' r$.

It was observed from Fig. 3(b) that like dielectric constant (ε), dielectric loss ($tan\ \delta$) also decreases exponentially withincrease in frequency. This decrease of tan δ with increase in frequency was due to the factthat there is a strong association between the dielectric behavior of the ceramics and the conduction mechanism [19, 20].Further, the decrease of tan δ with increasing frequency is attributed to the fact that the frequency of charge carriers cannot follow the changes to the externally applied electric field beyond a certain frequency limit. The *tan δ increases* with increase in Fe content *x*.

ISSN: 2005-4262 IJGDC

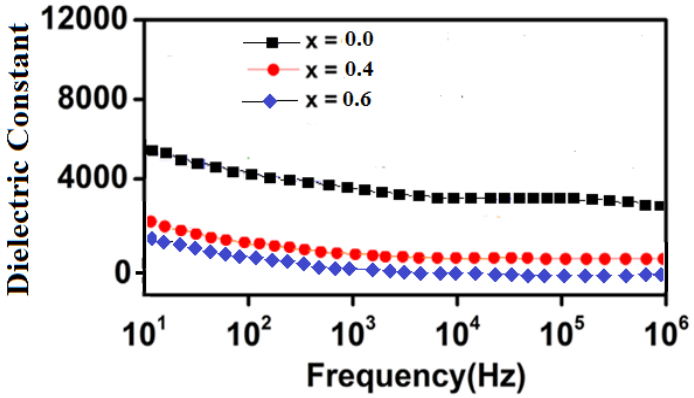

Fig. 3. (a) Variation of real part of relative dielectric constant as a function of frequency for $BaTi_{1-x}Fe_xO_3$ (x =0.0, 0.4,0.6) ceramics at room temperature.

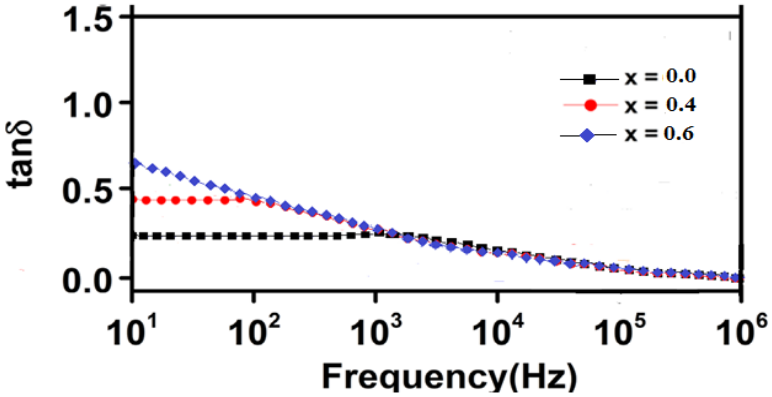

Fig. 3 (b) Variation of Dielectric loss (tan δ) as a function of frequency for $BaTi_{1-x}Fe_xO_3$(x = 0.0,0.4,0.6) ceramics at room temperature.

The variation of dielectric constant with an applied magnetic field is called Magnetodielectric (MD) effect [20-21]. This is due to magneto electric (ME) coupling between ferroelectric and ferromagnetic domains. The MD constant is defined as $[(\varepsilon r(H) - \varepsilon r(0))/\varepsilon r(0)] \times 100$, where $\varepsilon r(H)$ and $\varepsilon r(0)$ are dielectric constants with and without external magnetic field, respectively.Figure4 shows variationof MD constant (%) of$BaTi_{1-x}Fe_xO_3$ (x = 0.4,0.6) ceramics as a function of an appliedmagnetic field at room temperature.It is clear from Fig. 4 that the value of magneto dielectric coefficient increases continuously up to the 9kOe applied magnetic field. This observed magnetodielectric behavior may be due to the coupling between ferroelectric and magnetic domains. The magnetic domain in material is strained by the application of applied magnetic field. There after the strains induce a stress which in turn generates an electric field on the ferroelectric domain.According toGinzburg–Landautheory[21], the difference of the relative dielectric constant $\Delta\varepsilon$ will be proportional to the square of the magnetic-order parameter, i.e$\Delta\varepsilon - \gamma M^2$. The signof $\Delta\varepsilon$ depends on the sign of the magneto dielectric interaction constant(γ) . In Fe doped $BaTiO_3$ ceramics the MD coefficient is around 0.37 and 0.41 for x=0.4 and x=0.6 respectivelyat 9kOe.

ISSN: 2005-4262 IJGDC

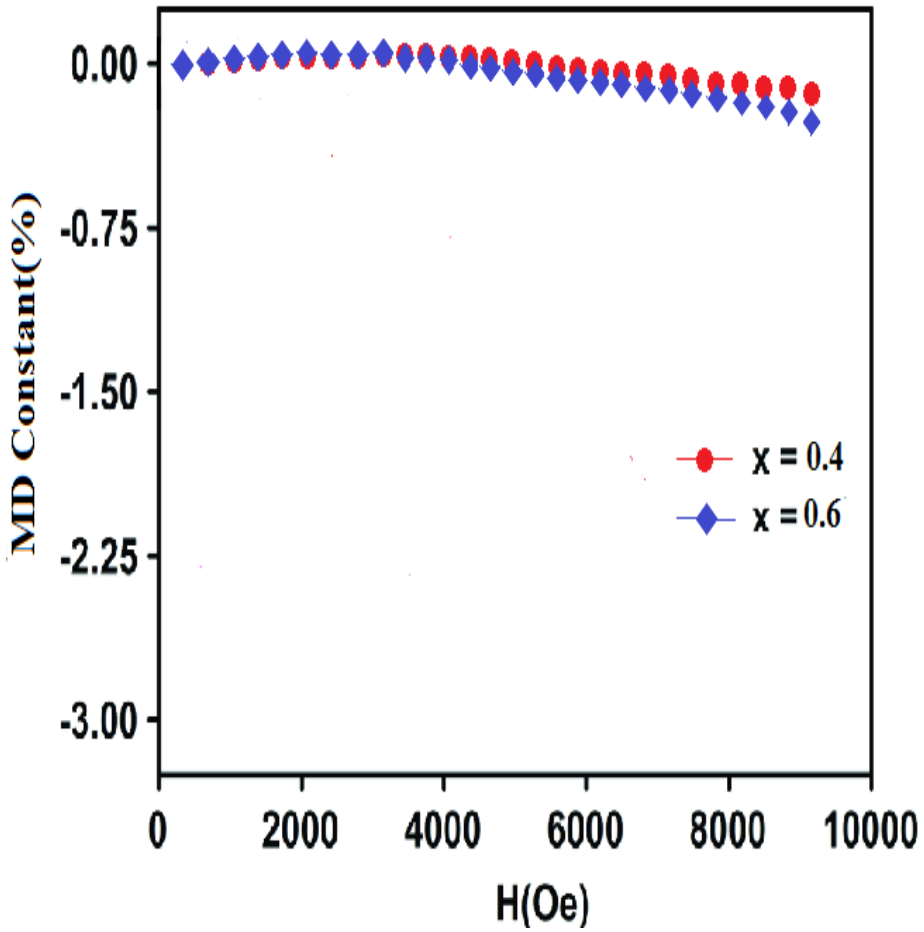

Fig. 4. Variation of MD coefficient with magnetic field for $BaTi_{1-x}Fe_xO_3$ (x = 0.4,0.6) ceramics

Conclusions:

The samples $BaTi_{1-x}R_xO_3$(wherex=0.0,0.4,0.6,) was prepared by solid state reaction method. X-ray diffraction analysisrevealed that phase transformation from tetragonal to hexagonaltake place at x=0.4. The lattice parameters (*a* and *c*) were observed to be increased linearly with Fe doping obeying the Vegard's law. The average crystallite size, lattice parameter, unit cell volume, micro-strain and texture coefficient value changes when Fe ions are doped in BaTiO3 lattice, resulting in the structural variation.In all Fe- doped BT samples,the grains exhibited rectangular and hexagonal shape. The average grain size were increased from1.6 to 3.0µm with increasingthe Fe content from x=0.0 to x=0.6. The dielectric constants of Fe-doped $BaTiO_3$ multiferroic ceramics exhibited a decrease with Fe concentration. This may be due to the less polarizability of Fe ion as compared to Ti ion. The decrease of dielectric losswith increasing frequency is attributed to the fact that the frequency of charge carriers cannot follow the changes to the externally applied electric field beyond a certain frequency limit.MD constant occurs due to strain mediated magneto electric coupling.MD coefficient measurements confirmed the ME coupling in Fe-doped $BaTiO_3$.

References:

1. S. E. Park and T.R. Shrout, J.Appl.Phys.82,1804(1997).
2. M.Ozgul,E.Furman,S.Trolier-McKinstry,andC.A.Randall,J.Appl.Phys. 95,2631(2004).
3. V.Born and,S.TrolieMcKinstry,K.Takemura,andC.A.Randall,J.Appl.Phys.87,3965 (2000).

ISSN: 2005-4262 IJGDC

4. X.Qi, J.Zhou, B.Li,Y.Zhang, Z.Yue,Z.Gui, and L.Li,J.Am.Ceram.Soc. 87 (2004)1848.
5. W.M. Zhua, H.Y.Guoa, and Z. G.Ye, J.Mater.Res.22 (2007) 2136.
6. H. Zheng, J.Wang, S. E. Lofland, Z.Ma, L.Mohaddes-Ardabili,T. Zhao, L.Salamanca-S.R.Shinde,S.B.Ogale,F.Bai,D.Viehland,Y.Jia,D.G.Schlom,M.Wuttig,A.Roytburd,and R.Ramesh,Science303 (20040)661.
7. H.A.Begum,H.Naganuma,M.Oogane,andY.Ando,Materials4 (2011)1087.
8. E.L.Colla,I.Stolichnov, P.E.Bradely,and N.Setter,Appl.Phys.Lett.82 (2003) 1604.
9. S.Valencia, A.Crassous, L.Bocher, V.Garcia, X.Moya, R.O.Cherifi ,C. Deranlot, K. Bouzehouane, S.Fusil ,A.Zobelli, A.Gloter, N.D.Mathur, A.Gaupp, R.Abrudan, F. Radu, A.Barthe´le´my, and M.Bibes,NatureMater.10 (2011) 753.
10. J.Zhang,J.Zhai,andX.Yao, Scr.Mater.61(2009) 764.
11. S. F.Wang,Y. C.Hsu,J.P.Chu,andC.H.Wu, Appl.Phys.Lett.88(2006) 042909.
12. T.Chakraborty,S. Ray,andM.Itoh,Phys.Rev.B83(2011) 144407.
13. A. Jana and T. K. Kundu, Mater Lett, 61 (2007) 1544.
14. E. Duverger, B. Jannot, M. Maglione and M. Jannin, Solid State Ionics, 73(1994) 139.
15. Suryanarayana C and Grant Norton M, X-Ray diffraction, a practical approach,(Plenum Press New York and London), 1998.
16. P. Yung, L. Jae Won and Kim Ho Gi, J. Phys.Condens. Matter, 9 (1997) 9445.
17. N. Maikhuri, A.K.Panwar and A.Jha, J.Appl.Phys.113(2013)17D915.
18. J. Rodríguez- Carvajal, Phys. B: Condens.Matter192 (1993) 55–69.
19. R.D. Shannon,ActaCrystallogr.Sect.A:Cryst.Phys.Diffr.Theor.Gen.Crystallogr.32 (1976)751–767.
20. G. Catalan, arXiv preprint cond- mat/0510313, (2005).
21. D. Wang, W.Goh,M. Ning, C.Ong, Appl.Phys.Lett.88(2006)2907.

ISSN: 2005-4262 IJGDC